Deformation Measurement of Highway Bridge Head Based on Mobile TLS Data

MAOHUA LIU[ID]1, XIUBO SUN[ID]2, YAN WANG[ID]1, YUE SHAO[ID]3, AND YINGCHUN YOU[ID]1

[1]School of Transportation Engineering, Shenyang Jianzhu University, Shenyang 110168, China
[2]Shenyang Center of Geological Survey, China Geological Survey, Shenyang 110168, China
[3]Liaoning Hongtuchuangzhan Surveying and Mapping Co. Ltd., Shenyang 110168, China

Corresponding author: Yue Shao (cemhliu@sjzu.edu.cn)

ABSTRACT The precise leveling method is often used to monitor the uneven deformation of the highway bridge head, which requires manual contact, dangerous and heavy workload. In order to solve these issues, this paper proposes a method to extract deformation features of the highway bridge head based on mobile terrestrial laser scanning (TLS) point clouds. Firstly, an automatic data acquisition system is designed to analyze and determinate the scanning station spacing and scanning resolution. Then acquired road point clouds are denoised based on the plane fitting method, which usually sets the experimental threshold. The road dividing line information is used for point clouds coarse registration, and the weighted average elevation method is used for refined registration. Lastly, the elevation of the deformation monitoring point is the average elevation of all points in the selected grid surface, which will mitigate random errors in the elevation of a single point. Point clouds of three different roads were collected to verify the proposed method. The results show that the accuracy of the elevation repeatability is better than ± 1mm, and the accuracy of the elevation check with the TM50 total station is better than ± 2mm, which meets the requirements of deformation monitoring. In addition, it takes about 3-4 minutes to complete the data collection of a station on the highway bridge head. Therefore, the proposed method based on mobile TLS data can be suitable for highway bridge head deformation measurement.

INDEX TERMS Terrestrial laser scanning (TLS), highway bridge head, deformation monitoring, automatic data acquiring system, point cloud processing.

I. INTRODUCTION

The highway bridge head is prone to uneven settlement during long-term use, and it is easy to bump when the vehicle passes at high speed, which seriously affects the safety of driving. Therefore, it is necessary to regularly monitor the uneven settlement of the highway bridge head. At present, the precise leveling method is usually used to monitor the settlement, which has high accuracy. However, when using this method, operators are required to work in the emergency lane and the personal safety of the operators cannot be effectively guaranteed [1], [2].

Obtaining a more complete model of the road, terrestrial laser scanning (TLS) overcomes the limitation of traditional surveying technologies, which measures only a few

The associate editor coordinating the review of this manuscript and approving it for publication was Abdel-Hamid Soliman[ID].

feature points. Furthermore, owing to the characteristic of non-contact measurement and high spatial resolution in a minimal amount of time-consuming, the application of TLS in the deformation monitoring of the highway bridge head will have significant technical advantages [3]–[6].

However, affected by the field environment, the obtained road point clouds have inevitable outliers. Therefore, one of the most important tasks is to eliminate outliers. Many scholars have done in-depth research in this area. Zhang *et al.* [7] propose an ellipse fitting algorithm based on the minimum P-norm of the residuals, and introduce an adaptive threshold to denoise the tunnel point cloud. Experimental results show that the algorithm has better robustness. Lipman *et al.* [8], Fleishman *et al.* [9], Dey and Sun [10] propose robust MLS (RMLS), adaptive MLS (AMLS) and data dependent MLS (DDMLS) to improve the moving least squares (MLS), respectively, which have better feature

retention while denoising. Zaman *et al.* [11] adopt the idea of clustering to classify the point cloud data, and then select the target subject on the clustering result to achieve point cloud denoising. However, these algorithms are usually complicated, time-consuming due to differential equations construction, polynomial fitting performing and so on. Therefore, it is necessary to investigate a more efficient denoising algorithm for point clouds of highway bridge head.

In order to unify the coordinate system of point clouds scanned from different stations, it is necessary to register the point cloud data. The conventional registration method is to set the target as a feature point for registration around the scanning field [12], but this method is limited to the operating scene, and especially not suitable for non-contact requirement of highway settlement measurement. Zhang [13] propose a registration method based on geographic scene, which adopts a three-step registration scheme of sequence stitching, global matching and data fusion, which can better meet the registration needs of special geographic scenes. Zhang *et al.* [14] propose a robust algorithm for point cloud registration based on the characteristics of building planes, and compare with iterative closest point (ICP) method, proving that the algorithm is effective. Zhu and Davari [15] investigate the efficiency of registration of different feature combinations for 3D architectural scenes. 31 actual scenes show that the scale-invariant feature matching method is more accurate. However, there are few obvious geographic or architectural features in highway and any two site clouds are very similar, which make the ICP registration method unsuitable for highway point cloud registration. In addition, some novel and effective algorithms for planar registration and segmentation have been proposed recently [16]–[18], such as unsupervised robust planar segmentation, procedural shape priors-based building facades segmentation and a multiscale tensor voting method. Especially, Wu *et al.* [18] improve the selection of seed points in region-growing algorithm and obtain comprehensive planar segmentation results, which are more robust than clustering-based methods. Yet, the uneven deformation monitoring of the highway bridge head requires lower plane accuracy, which is generally about ±2cm, and higher elevation accuracy, which is generally better than ±5mm [19]. Therefore, considering the special requirements of the highway bridge head deformation monitoring and computational loads, an improved registration method needs to be further studied.

In addition, extracting the monitoring point elevation based on the processed point clouds is an important step for deformation monitoring. Roberts and Matthew [20] use TLS point clouds to extract the deformation information of the concrete beams of the building, and check with a total station, finding that the accuracy is the same in the range of 3-35m. Zogg and Ingensand [21] conduct a viaduct load test using TLS, showing that the difference between TLS and precision level is less than 1mm, indicating that TLS can achieve millimeter-level deformation monitoring. Lõhmus *et al.* [22] monitor the vertical deformation of the two bridges by TLS

and find that the average difference with the precision level method is about 2 mm, which can be used as a supplement to the precision level method. Most of the above researches focus on the deformation monitoring of reinforced concrete structures with regular shape, but less research on highway bridge head, whose surface features are not regular.

The paper aims to extract deformation information of highway bridge head based on mobile TLS point clouds. In Section 2, the data acquisition system and its implementation are described in detail. Then, the point cloud processing and deformation extraction are described in Section 3. The Section 4 presents three different scenarios to verify the proposed method. The conclusion is given in Section 5.
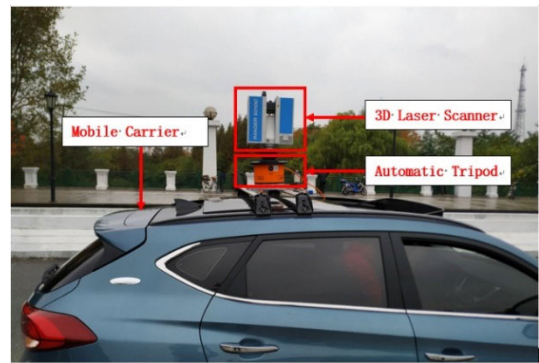
(a) The hardware composition of the mobile scanning system
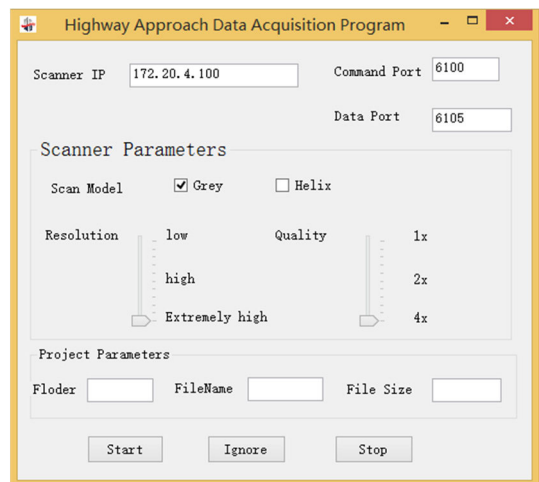
(b) Data acquisition configuration interface of the mobile scanning system

FIGURE 1. **The mobile scanning system.**

II. INSTRUMENTS AND DATA COLLECTION
A. INSTRUMENTS
In order to efficiently collect point clouds of highway bridge head, a mobile vehicle scanning system is designed in this paper, which will prevent operators from getting out of the vehicle and improve the safety factor. The hardware and software interface of the system is shown in Figure 1. As shown in Figure 1, the mobile scanning system is mainly composed

of a three-dimensional laser scanner (Z + F), a mobile carrier, a fixed frame, and an automatic leveling base. The Z+F Image 5010c is amongst the fastest 3D laser scanner in the market [23].

The scanner and the auto-leveling base are fixed on the roof of a car through a fixing frame, which can realize the real-time automatic leveling of the scanner. The data acquisition software has been developed, which will facilitate the control of the scanner in the car. The main functions of the data acquisition software include project settings, scanning parameter settings, and point clouds preview. The communication with the scanner is realized through wireless local area network (WLAN), and the corresponding IP address and port are set through the software. The project settings mainly include the scan data storage path, scanning file name, and the scanning parameter settings mainly include the scanner's acquisition resolution, quality, and acquisition mode. At the end of the scan task, the software automatically pops up a preview interface of the point clouds. The point clouds are collected in a stop-and-go operation mode, which makes the motion carrier remain stationary every certain distance. After the current scanning is completed, the carrier moves forward according to a preset distance, and continues to get road point cloud data. The above steps are repeated until all the roads to be detected are scanned. In order to improve the data collection efficiency and ensure the accuracy of the point clouds, reasonable station spacing and scanner parameters are very important [24], [25].

B. STATION SPACING

Due to the limitation of the field of view and the ranging range, multiple stations need to be arranged on the highway for scanning separately. The larger the distance between the stations, the fewer the total number of stations required, and the shorter the scanning time. However, an excessively large distance between the stations will lead to a reduction in the quality of the point cloud data, which is caused by an excessively large incident angle of the laser on the ground. Incident angle refers to the angle between the emission direction of the laser and the normal to the surface of the scanning target. The larger the incident angle of scanning, the greater the measurement error [21]. The basic principle is shown in Figure 2.
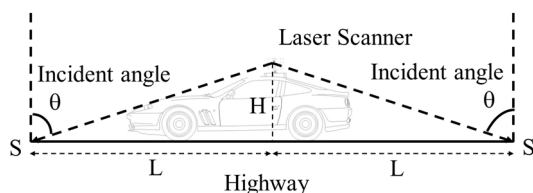

FIGURE 2. Geometrical relationship between the scanning system and road.

As shown in Figure 2, the largest incident angle is located at the point S, and the geometric relationship between the station distance ($2L$), the scanner height (H), and the maximum

incident angle (θ) can be expressed as:

$$\theta = arctan \frac{L}{H} \qquad (1)$$

Lichti [26] show that when the incident angle is greater than 75°, the scanning error starts to rise sharply. According to Equation (1), when θ is less than 75°, L is less than $3.7 * H$. The height of the scanner from the ground is about 2.2 m, so L $\approx$ 8.2 m, and the station spacing can be set to 16m.

C. SCANNER PARAMETERS

The scanner parameters mainly include scanning resolution, scanning quality, scanning initial attitude, scanning time, etc. This section focuses on analyzing the settings of scanning resolution and scanning initial attitude.

The resolution of Z + F scanner has 6 levels, including "low, middle, high, super high, ultra-high, extreme high". The higher the resolution, the higher the density of the point cloud. The higher density reveals the clearer the details of the scanned object, however, the more time which takes to scan. Dot spacing, scan time and angular step for different resolutions of Z + F scanner are shown in Table 1.

TABLE 1. Scanning information at different resolutions at 16m station spacing.

Resolution	Dot Spacing(mm)	Scan Duration(minute)	Angular Step(second)
low	20.4	0:52	527
middle	9.8	1:44	253
high	6.1	3:22	158
super high	4.9	6:44	126
ultra-high	2.5	13:28	63
extreme high	1.2	81:00	32

Notes: scan duration time is in normal quality condition.

As mentioned above, the optimal station spacing is 16m, that is, the maximum distance between the target point and the scanner is 8m. In addition, according to the needs of data processing, the dot spacing should be no more than 5mm. Therefore, in order to ensure the highest scanning efficiency, "Super high" resolution can be used.

Proper scanning initial attitude is conducive to data processing. To facilitate the denoising of point cloud data, the *X* axis of the scanner is set to be parallel to the road and point in the forward direction; the *Y* axis of the scanner is set to be perpendicular to the road; the Z axis, X axis and Y axis are perpendicular to each other and finally form a right-handed system. The geometric relationship between the scanning coordinate system and the road is shown in Figure 3.

III. METHODOLOGY

Because point clouds are massive and scattered, it is the key to obtain true and reliable deformation information of highway bridge head from massive and scattered point clouds. This section focuses on three key issues: point clouds denoising, point clouds registration, and deformation information extraction.
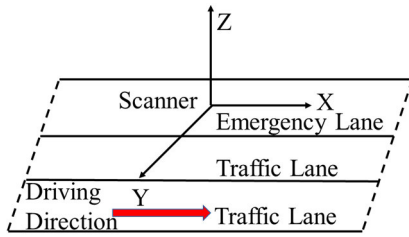
FIGURE 3. Definition of the scanning coordinate system.

A. POINT CLOUDS DENOISING

The noises in the road point clouds collected by the three-dimensions (3D) laser scanner mainly include passing vehicles, green vegetation, street lights, and airborne noise. These noises can not only increase the number of point clouds, but also seriously affect the processing and analysis of point clouds. According to the spatial distribution of point clouds, these noises can be mainly divided into two categories: (1) drifting points: significantly away from the main body (2) mixed points: confused with the correct point clouds. The first type of noise is irrelevant to the road surface and far from the main part of the road, whereas the second type of noise is related to the road and mixed with the main point cloud of the road surface, as shown in Figure 4. The point clouds were collected from a real highway experiment, which will be described in next section.
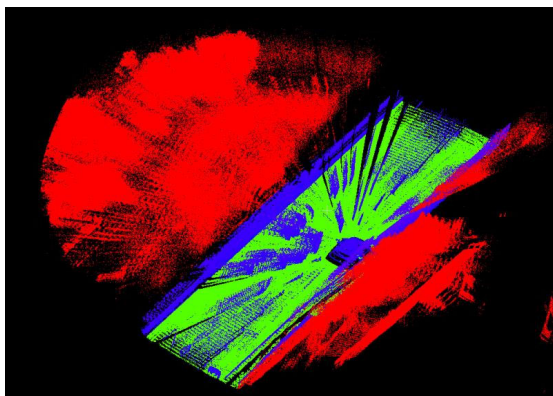

FIGURE 4. The original point clouds of highway bridge head before denoising. The red points are type (1), the blue points are type (2).

Since the initial scanning attitude is set during data acquisition, the following formula can be used for rough noise elimination:

$$-\alpha * D < X < \alpha * D, \quad -L < Y < n * L,$$
$$H - h < Z < H + h \quad (2)$$

where X, Y, Z are the coordinates of the point cloud, D is the distance between two adjacent stations, α is the point cloud denoising adjustment coefficient, L is the width of each lane, n is the number of driving lane, H is the height of the scanner from the ground, h is the height error of H. Considering the

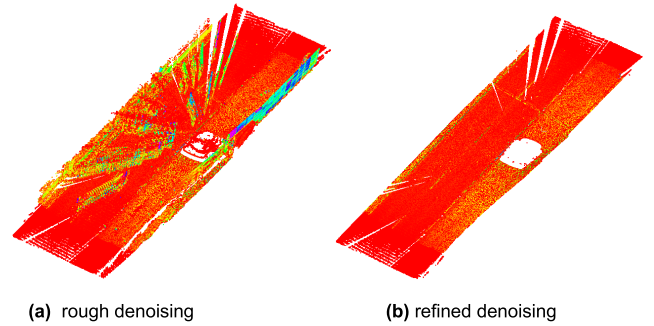(a) rough denoising   (b) refined denoising

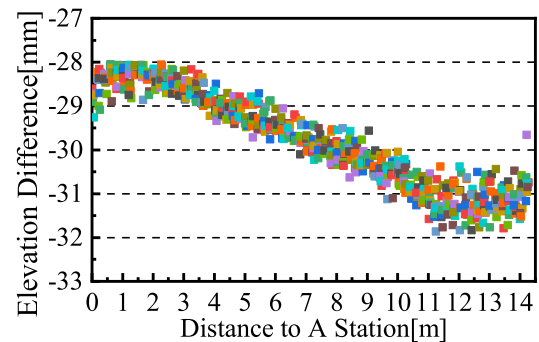FIGURE 5. Denoising of the point clouds of highway bridge head.

FIGURE 6. The elevation difference sequence of the common point.

number of single-site clouds and denoising efficiency, we can empirically take α equal to 0.8. According to national code for design of road engineering [27], the lane width is 3.75 m. Taking into road construction errors, we take L as 4.0 m in this paper. In addition, because the scanning operation is usually on the emergency lane, the Y value should be greater than negative L and less than n times L. The H value of the scanner is about 2 m and the height error caused by the road slope is taken as 0.2 m based on national code for design of road engineering [27]. The point clouds are roughly denoised as shown in left subplot of Figure 5. As can be seen from left subplot of Figure 5, there are still a lot of noise points in the middle of the road. Therefore, further fine denoising is needed. As the road surface is approximately an inclined surface, the plane fitting of point cloud based on random sampling consistency is adopted to obtain the plane parameters [28], which are a,b,c,d. Then we can compute the vertical distance from each point to the fitting plane:

$$V_i = \frac{|aX_i + bY_i + cZ_i + d|}{\sqrt{a^2 + b^2 + c^2}} \quad (3)$$

where i is the point, V_i is the distance of the point to the fitting plane. Then we can calculate the average value of V_i the values at all points:

$$V_{mean} = \frac{\sum_i^n V_i}{n} \quad (4)$$

When V_i is greater than two times the V_{mean} value, this point is removed as outlier. The refined denoising point clouds are shown in right subplot of Figure 5.
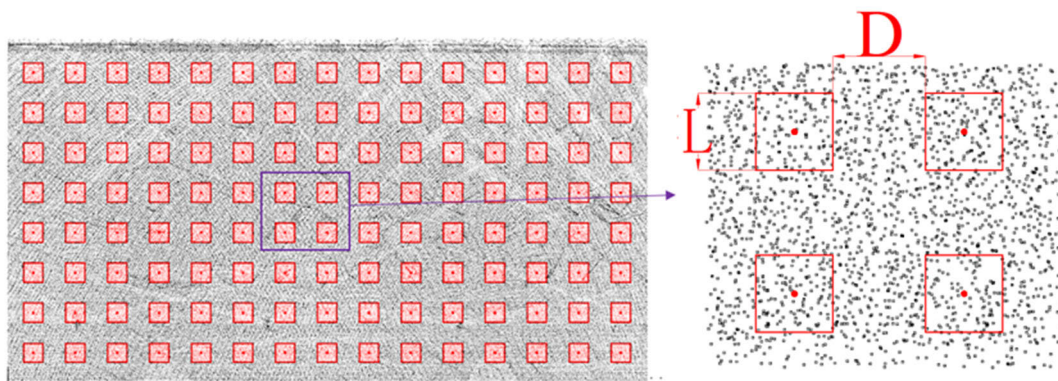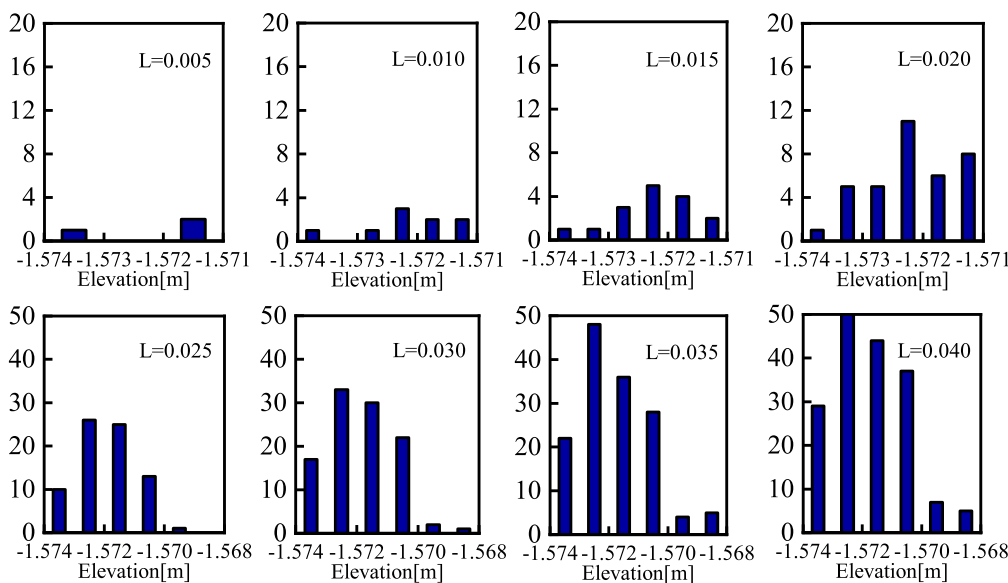
FIGURE 7. Layout of detection point distribution.

FIGURE 8. Elevation statistical distribution map of different *L* values.

B. POINT CLOUDS REGISTRATION

For the settlement monitoring of highway bridge head, the method of non-contact measurement is required. Therefore, it is not feasible to place feature points, such as target balls. In addition, the characteristics of highway bridge head point clouds are not obvious, and the clouds of any two sites are very similar, which make the ICP registration method not suitable for point clouds of highway bridge head. So, a new step-by-step registration algorithm for point clouds of highway bridge head is proposed in this section.

1) PLANAR REGISTRATION

Planar registration method utilizes conventional feature points to align [29], [30]. Supposing scanned at A station and B station, respectively, point clouds named P in the coordinate system $O_1 - x_1y_1z_1$ are obtained at station A, and point clouds named Q in the coordinate system $O_2 - x_2y_2z_2$ are obtained at station B. We adopt the common feature points

of the two site clouds, such as the corner points of traffic signs, the center of the guardrail cylinder, etc. Let the feature point set of station A be P_T, and that of station B be Q_T. The feature point sets $P\_T(X, Y)$ and $Q\_T(x, y)$ satisfy the equation:

$$\begin{pmatrix} X \\ Y \end{pmatrix} = R \begin{pmatrix} x \\ y \end{pmatrix} + \begin{pmatrix} \Delta X \\ \Delta Y \end{pmatrix} \qquad (5)$$

where R is the rotation matrix, ΔX and ΔY are the translations in the X and Y directions. Assuming that α and β are rotation angles, respectively, the rotation matrix can be expressed as:

$$R = \begin{bmatrix} cos\alpha & -sin\alpha \\ sin\alpha & cos\alpha \end{bmatrix} \begin{bmatrix} cos\beta & -sin\beta \\ sin\beta & cos\beta \end{bmatrix} \qquad (6)$$

Generally, constrained by the accuracy of feature point recognition, the plane registration accuracy is about 2 cm [31], [32]. As the accuracy of monitoring the uneven settlement of the

TABLE 2. The operation configuration of three experiments.

Content	Experiment one	Experiment two	Experiment three
Operating time	20-6-2019	20-11-2019	12-11-2019
Operating location	Municipal road	Highway(G1501)	Highway(G10)
Lane number	2	3	3
Station Spacing	16 m	16 m	16 m
Resolution	Super High	Super High	Super High
Quality Mode	Low	Low	Low
Scanning Range	~64 m	~70 m	~80 m
Scanning Time	~15 min	~20 min	~20 min
Scanning Stations	4	5	5
Round trip	Yes	Yes	Yes

FIGURE 9. Field environmental conditions of three experiments.

TABLE 3. Statistical results of elevation differences of every adjacent stations (in mm).

Experiment Number	Adjacent Station	Common Points Number	Max	Min	Mean	STD
One	Scan1-Scan2	2060	-17	-23	-20	1.2
	Scan2-Scan3	2210	18	12	15	0.9
	Scan3-Scan4	2420	-29	-35	-32	1.1
Two	Scan1-Scan2	3606	-26	-33	-29	0.9
	Scan2-Scan3	3703	-27	-33	-30	0.9
	Scan3-Scan4	3425	23	17	20	1.0
	Scan4-Scan5	3519	-19	-25	-22	1.1
Three	Scan1-Scan2	3980	27	23	26	0.4
	Scan2-Scan3	4500	16	10	13	1.5
	Scan3-Scan4	4626	-13	-19	-16	0.8
	Scan4-Scan5	4870	-26	-35	-32	1.1

highway bridge head is required to be within $\pm$ 5mm, this paper proposes a weighted elevation alignment algorithm based on common points for the alignment of elevation data.

2) VERTICAL WEIGHTED REGISTRATION

Due to the accurate leveling of the scanner, theoretically the cloud data height difference between the two stations is a constant. By selecting the two-site cloud public area, we can calculate the two-site cloud elevation difference.

The point clouds at station A overlapping with station B are recorded as *PA*, the distances between *PA* and the scanning center of station A are recorded as *D_PA*, and the elevations of *PA* are recorded as *H_PA*. The point clouds at station B overlapping with station A are recorded as *PB*, the distances

between *PB* and the scanning center of station B are recorded as *D_PB*, and the elevations of *PB* are recorded as *H_PB*. Therefore, the elevation difference between *PA* and *PB* is:

$$\Delta H = H\_PA - H\_PB \tag{7}$$

where ΔH is the elevation difference. Figure 6 shows the elevation difference sequence of the common point of station A and station B, whose point clouds are collected from the Experiment two. The two adjacent stations are Scan 2 and Scan 3.
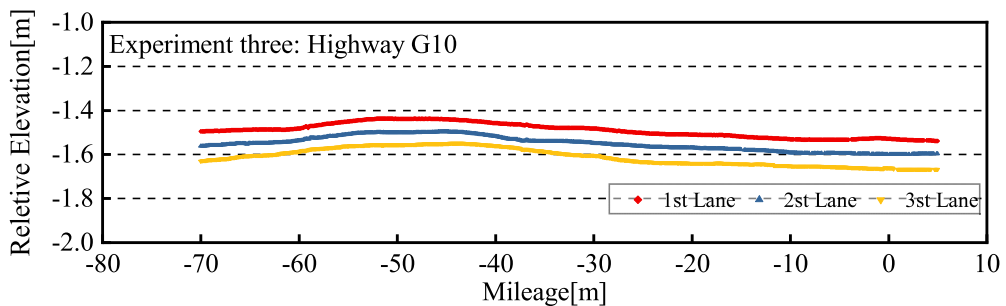
As can be seen from Figure 6, the elevation difference between the common points of the two stations varies from -28 mm to -32 mm. This is mainly caused by the instrument shafting and leveling errors. In order to reasonably calculate
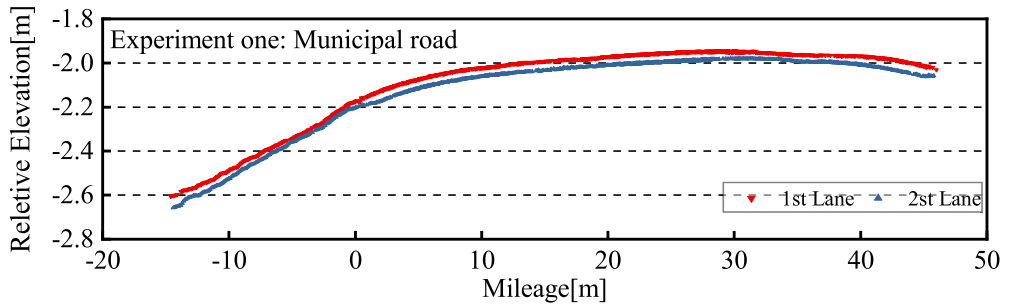
(a) Elevation changes of two lanes in a municipal road bridge head.
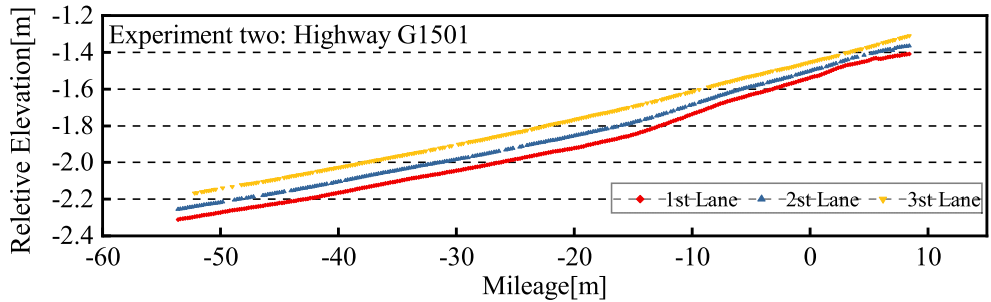
(b) Elevation changes of three lanes in G1501 highway bridge head.

(c) Elevation changes of three lanes in G10 highway bridge head.

FIGURE 10. **Elevation changes of different lanes. Here we use the relative elevation based on a reference plan.**

the elevation difference of the scanning station, a distance-based weighting method is introduced. Taking into account the distance between the common point i and scanning station, the weight of ΔH_i can be determined as:

$$P_i = \sqrt{\frac{\left(\frac{MD_{PA}-D_{PA}}{MD_{PA}}\right)^2 + \left(\frac{MD_{PB}-D_{PB}}{MD_{PB}}\right)^2}{2}} \quad (8)$$

where MD_{PA}, MD_{PB} are the maximum distances of the public point cloud from the station A to station B, D_{PA}, D_{PB} are the distances of the point i from the station A to station B. Taking the weighted average value of the elevation differences of all common points as the actual elevation difference between the two station, that is:

$$\Delta H = \frac{\sum P_i \Delta H_i}{\sum P_i} \quad (9)$$

Based on the weighted height difference between the two stations, we achieve registration in the vertical direction and eliminate the stratification phenomenon.

### C. DEFORMATION INFORMATION EXTRACTION

When using traditional leveling method to monitor the highway bridge head, several leveling points are arranged in sequence only at the edge of the emergency lane, and the spacing between the leveling points is generally about $3 \sim 5$ m. However, when TLS method is used, a full coverage of the road can comprehensively indicate the elevation change information of the road. In this paper, a detection point is extracted every certain distance along the longitudinal direction and transverse direction of the road. The longitudinal (road extension direction) starting point is the joint between the road and the bridge, and the transverse starting point is the edge of the emergency lane. After the plane position of the
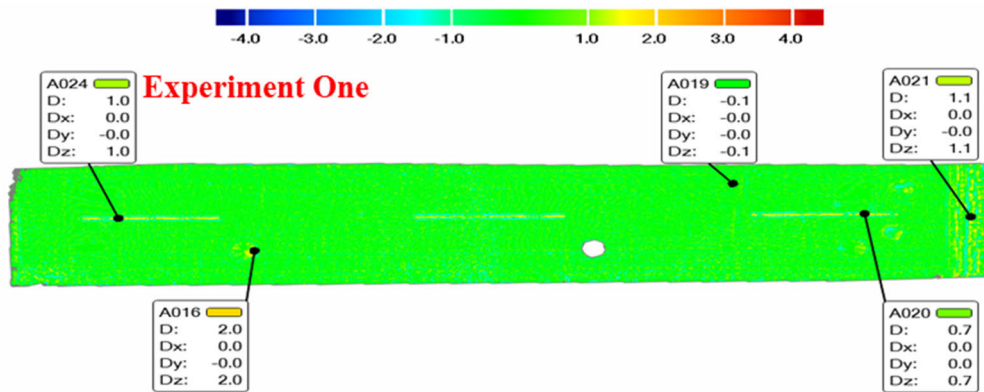
(a) Elevation differences between the round-trip scans in a municipal road bridge head.
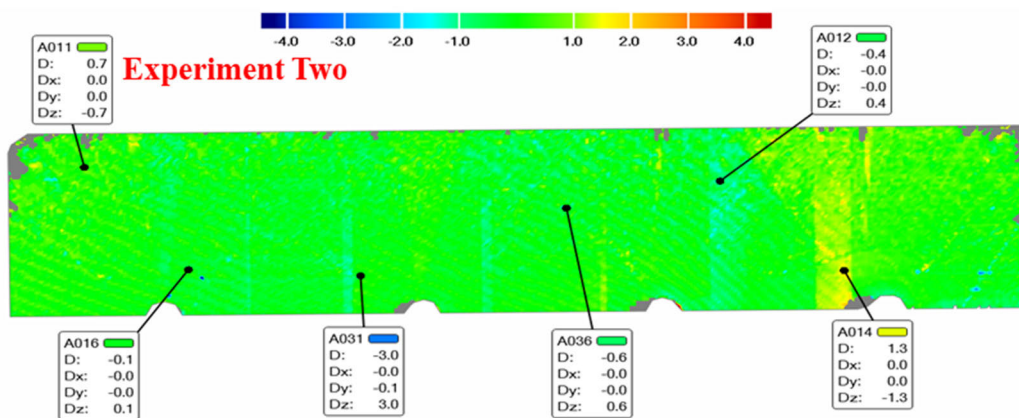
(b) Elevation differences between the round-trip scans in G1501 highway bridge head.
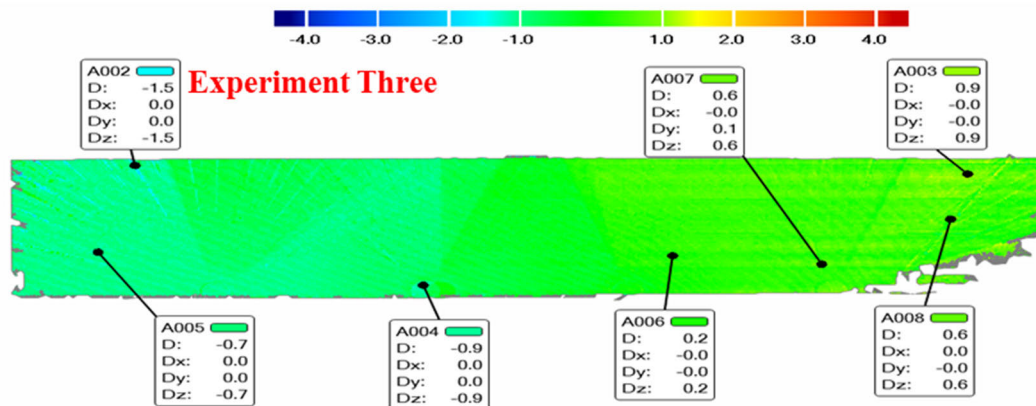
(c) Elevation differences between the round-trip scans in G10 highway bridge head.

FIGURE 11. The chromatogram of elevation differences between the round-trip scans. The unit is mm.

detection points are determined, we can calculate the elevation of each detection point. Because there is a large random error at a single point, we extract the elevation information by the average elevation of all points in the selected grid surface, as shown in Figure 7.

As shown in Figure 7, the *D* value determines the distance between adjacent detection points, which can be determined according to actual needs. *L* has a greater impact on the accuracy of elevation extraction. If the value of *L* is too large, the surface selected by the square frame may be an

inclined surface, and the elevation of the center point cannot be obtained. If the value of L is too small, the number of points selected by the square frame is insufficient to prevent the effect of gross errors. Therefore, choosing a reasonable L value is very important. When different L values are selected, there is a difference in the elevation distribution of the points within the square frame, as shown in Figure 8.

It can be seen from Figure 8 that when L is less than 0.02 m, the number of points in the area is small, and the point elevation fluctuation is small, but the distribution is irregular; when L is more than 0.02 m, the number of points in the area is large, but the point elevation is fluctuating. Taking all factors into consideration, we will take L as 0.02 m. Since the elevations of the points in the area basically follow the normal distribution, the average elevation value of all points is used as the elevation of the detection points.

## IV. RESULTS AND DISCUSSION

In order to verify the feasibility of the method in this paper, three experiments were conducted. The first experiment was conducted on a municipal road and was used to initially evaluate the stability of the data collection and processing. The last two experiments were conducted on two different highways and were used to assess the effectiveness of the method in the real environment. The specific details of the three experiments are shown in Table 2 and field environmental conditions are shown Figure 9. Therefore, we can calculate that the operation time of each station is about 3-4 minutes.

After collecting point clouds, the rough and refined denoising are conducted by proposed method and the result is shown in Figure 5. Considering the similarity of denoising, we only give the denoising results of Experiment two. When the denoising is completed, the planar registration is based on the corner points of the road dividing line, and then the elevation registration is based on the public point cloud. The statistical results of the elevation difference between all two adjacent stations are shown in Table 3.

It can be seen from Table 3 that there are more common points in experiment two and three than that in experiment one, which is because that the first has only 2 lanes and the last two have 3 lanes. In addition, the average standard deviation (STD) of all stations is about 1mm, which indicates that the point cloud registration method is feasible.

Then, the deformation information acquisition method described in section 3.3 is used to extract the elevation of each lane, which are shown in Figure 10. The X axis represents the mileage of the longitudinal section of the road, and its starting point is determined according to the convenience of measurement and location of the joint between the road and the bridge. The Y axis represents the elevation change of the longitudinal section of the road. As can be seen from Figure 10, the elevation changes of different lanes on the same road are basically the same, which macroscopically shows the feasibility of extracting elevation information.
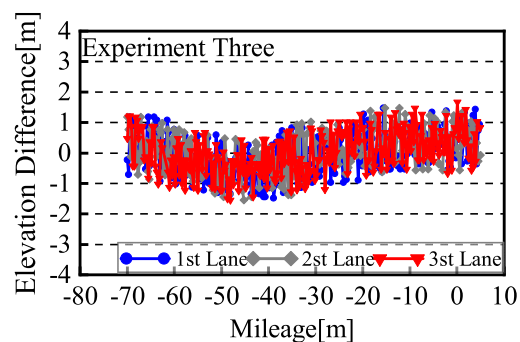
In order to verify the internal coincidence accuracy of the detection method in this paper, the same method and the same
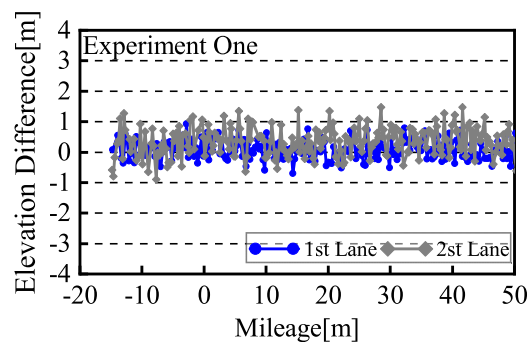
(a) Elevation differences statistics in Experiment one.
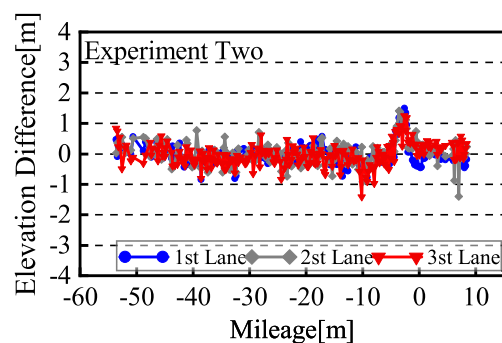
(b) Elevation differences statistics in Experiment two.

(c) Elevation differences statistics in Experiment three.

FIGURE 12. Statistics of elevation difference between round-trip scans based on extracted points.

parameters were used for round-trip scanning. At the same time, four reference targets are arranged at both ends to unify the coordinate system of the round-trip data. The round-trip comparison results are shown in Figure 11. Figure 11 depicts the chromatogram of the difference between round-trip scans. The corresponding relationship between the difference and the color is plotted in the figure. It can be seen from the figure that the comparison results of the round-trip scans are overall greenish, that is, the difference is less than ± 1 mm, and a light blue or light-yellow color appears in a small range, that is, the difference is greater than ± 1 mm and less than ± 2 mm.

In order to quantify the comparison results of the round-trip scans, according to the method in section 3.3, some points are extracted for each lane. The elevation difference of the

TABLE 4. Statistics of elevation differences between TLS method and Total station method (in mm).

	Row Number	Mean	STD
Experiment two	Row1	0.07	1.20
	Row2	-0.30	1.11
	Row3	-0.24	1.38
	Row4	-0.59	1.68
Experiment three	Row1	-0.42	1.32
	Row2	0.18	1.02
	Row3	0.35	1.28
	Row4	-0.47	1.46

same detection point is compared, and the results are shown in Figure 13. It can be seen from Figure 12 that most elevation differences for three experiments are within ±1 mm, and average height differences of all lanes are basically zero, which indicates that the repeat measurement accuracy is better than ±1 mm.

To further verify the accuracy of the method in this paper, the TM50 total station was used to collect 68 measurement points in Experiment 2 and Experiment 3 respectively, which are divided into four rows along the road. At the same time, four reference targets are arranged at both ends of the road to unify the coordinate system. According to the plane coordinates of the total station detection points, the same position points in the point clouds are compared with the total station data, and the comparison results are shown in Table 4. It can be seen from Table 4 that the mean value of the elevation difference of the four rows is less than ±1 mm, and the average is −0.2 mm; the maximum standard deviation is 1.68 mm, and the average standard deviation is 1.31mm, which indicates that the external accuracy of proposed method is better than ±2 mm.

V. CONCLUSIONS

The traditional precise levelling method for monitoring the uneven settlement of the highway bridge head has the disadvantages of high-risk coefficient, high-operation cost and single measurement result. In view of the above problems, this paper proposes a method for extracting the deformation information of the highway bridge head based on TLS point clouds, and gets the following results:

(1) According to the characteristics of mobile scanning, an automatic data acquisition system is designed, and its basic operation process is further discussed. Through the analysis of the scanning station spacing and scanner parameters, reasonable theoretical values are determined.

(2) An efficient and accurate denoising method for the highway bridge head point clouds is determined. According to the lane width, the height of the scanner, and the preset scanning attitude, we realize the coarse noise removing, and then use the plane fitting algorithm for accurate noise removing.

(3) The weighted elevation registration algorithm is used for refined registration, which effectively eliminates the feature point identification and random errors, and can achieves ±1 mm accuracy.

(4) Through three different experiments, it finds that the accuracy of round-trip measurement is better than ±1 mm, and compared with the total station measurement, the external check accuracy is better than ± 2mm, which meet the requirements of highway approach deformation monitoring.

ABBREVIATIONS

The following abbreviations are used in this manuscript:

TLS	Terrestrial laser scanning
MLS	Moving least squares
RMLS	Robust moving least squares
AMLS	Adaptive moving least squares
DDMLS	Data dependent moving least squares
ICP	Iterative closest point
WLAN	Wireless local area network
3D	Three dimensions
STD	Standard deviation

REFERENCES

[1] M. C. de Lacy, M. I. Ramos, A. J. Gil, Ó. D. Franco, A. M. Herrera, M. Avilés, A. Domínguez, and J. C. Chica, "Monitoring of vertical deformations by means high-precision geodetic levelling. Test case: The arenoso dam (South of Spain)," *J. Appl. Geodesy*, vol. 11, no. 1, pp. 31–41, Jan. 2017.

[2] Y.-Y. Lu, C.-Q. Ke, H.-J. Jiang, and D.-L. Chen, "Monitoring urban land surface deformation (2004–2010) from InSAR, groundwater and levelling data: A case study of Changzhou city, China," *J. Earth Syst. Sci.*, vol. 128, no. 6, p. 159, Aug. 2019.

[3] W. Wang, W. Zhao, L. Huang, V. Vimarlund, and Z. Wang, "Applications of terrestrial laser scanning for tunnels: A review," *J. Traffic Transp. Eng.*, vol. 1, no. 5, pp. 325–337, Oct. 2014.

[4] K. Tan, X. Cheng, Q. Ju, and S. Wu, "Correction of mobile TLS intensity data for water leakage spots detection in metro tunnels," *IEEE Geosci. Remote Sens. Lett.*, vol. 13, no. 11, pp. 1711–1715, Nov. 2016.

[5] T. Nuttens, "High resolution terrestrial laser scanning for tunnel deformation measurements," in *Proc. FIG Congr.*, 2010, pp. 1–15.

[6] V. Gikas, "Three-dimensional laser scanning for geometry documentation and construction management of highway tunnels during excavation," *Sensors*, vol. 12, no. 8, pp. 11249–11270, 2012.

[7] L. Zhang, X. Cheng, L. Wang, and X. Cheng, "Ellipse-fitting algorithm and adaptive threshold to eliminate outliers," *Surv. Rev.*, vol. 51, no. 366, pp. 250–256, May 2019.

[8] Y. Lipman, D. Cohen-Or, and D. Levin, "Data-dependent MLS for faithful surface approximation," in *Proc. 5th Eurograph. Symp. Geometry Process.*, 2007, pp. 59–67.

[9] S. Fleishman, D. Cohen-Or, and C. T. Silva, "Robust moving least-squares fitting with sharp features," *ACM Trans. Graph.*, vol. 24, no. 3, pp. 544–552, Jul. 2005.

[10] T. K. Dey and J. Sun, "An adaptive MLS surface for reconstruction with guarantees," in *Proc. Symp. Geometry Process.*, 2005, pp. 43–52.

[11] F. Zaman, Y. P. Wong, and B. Y. Ng, "Density-based denoising of point cloud," in *Proc. 9th Int. Conf. Robot., Vis., Signal Process. Power Appl.*, 2017, pp. 287–295.

[12] M. Scaioni, "Direct georeferencing of TLS in surveying of complex sites," in *Proc. ISPRS Work. Group*, vol. 4, 2005, pp. 22–24.

[13] Z. Kai, "Research on spatial registration of 3D laser scanning data," M.S. thesis, Nanjing Normal Univ., Nanjing, China, 2008.

[14] D. Zhang, T. Huang, G. Li, and M. Jiang, "Robust algorithm for registration of building point clouds using planar patches," *J. Surveying Eng.*, vol. 138, no. 1, pp. 31–36, Feb. 2012.

[15] Z. Zhu and K. Davari, "Comparison of local visual feature detectors and descriptors for the registration of 3D building scenes," *J. Comput. Civil Eng.*, vol. 29, no. 5, Sep. 2015, Art. no. 04014071.

[16] J. M. Biosca and J. L. Lerma, "Unsupervised robust planar segmentation of terrestrial laser scanner point clouds based on fuzzy clustering methods," *ISPRS J. Photogramm. Remote Sens.*, vol. 63, no. 1, pp. 84–98, Jan. 2008.

[17] O. Teboul, L. Simon, P. Koutsourakis, and N. Paragios, "Segmentation of building facades using procedural shape priors," in *Proc. IEEE Comput. Soc. Conf. Comput. Vis. Pattern Recognit.*, Jun. 2010, pp. 3105–3112.

[18] H. Wu, X. Zhang, W. Shi, S. Song, A. Cardenas-Tristan, and K. Li, "An accurate and robust region-growing algorithm for plane segmentation of TLS point clouds using a multiscale tensor voting method," *IEEE J. Sel. Topics Appl. Earth Observ. Remote Sens.*, vol. 12, no. 10, pp. 4160–4168, Oct. 2019.

[19] *Highway Performance Assessment Specification*, document TJ 08-2095-2012, 2012.

[20] R. Gethin and B. Matthew, "Deformation monitoring trials using a Leica HDS 3000," in *Proc. Pharaohs Geoinformat. FiG Work. WEEJ (GSDI)*, Cairo, Egypt, 2007, pp. 16–21.

[21] H.-M. Zogg and H. Ingensand, "Terrestrial laser scanning for deformation monitoring: Load tests on the Felsenau Viaduct (CH)," *Int. Arch. Photogramm., Remote Sens. Spatial Inf. Sci.*, vol. 37, pp. 555–562, Jul. 2008.

[22] H. Lõhmus, A. Ellmann, S. Märdla, and S. Idnurm, "Terrestrial laser scanning for the monitoring of bridge load tests–two case studies," *Surv. Rev.*, vol. 50, no. 360, pp. 270–284, May 2018.

[23] *Z+F IMAGER 5010C. 3D Laserscanner*. Accessed: Oct. 7, 2019. [Online]. Available: https://www.zf-laser.com/fileadmin/editor/Broschueren/Broschure_IMAGER_5010C_en_comp.pdf

[24] M. Barbarella, M. R. de Blasiis, and M. Fiani, "Terrestrial laser scanner for the analysis of airport pavement geometry," *Int. J. Pavement Eng.*, vol. 20, no. 4, pp. 466–480, 2019.

[25] T. Zemánek, M. Cibulka, P. Pelikán, and J. Skoupil, "The use of terrestrial laser scanning for determining the Driver's field of vision," *Sensors*, vol. 17, no. 9, p. 2098, 2017.

[26] D. D. Lichti, "Error modelling, calibration and analysis of an AM–CW terrestrial laser scanner system," *ISPRS J. Photogramm. Remote Sens.*, vol. 61, no. 5, pp. 307–324, Jan. 2007.

[27] *Code for Design of Road Engineering*, document CJJ37-2012, 2012.

[28] A. Nguyen and B. Le, "3D point cloud segmentation: A survey," in *Proc. 6th IEEE Conf. Robot., Autom. Mechatronics (RAM)*, Nov. 2013, pp. 225–230.

[29] C.-C. Lin, Y.-C. Tai, J.-J. Lee, and Y.-S. Chen, "A novel point cloud registration using 2D image features," *EURASIP J. Adv. Signal Process.*, vol. 2017, no. 1, pp. 1–11, Dec. 2017.

[30] D. Grant, J. Bethel, and M. Crawford, "Point-to-plane registration of terrestrial laser scans," *ISPRS J. Photogramm. Remote Sens.*, vol. 72, pp. 16–26, Aug. 2012.

[31] D. Zai, J. Li, Y. Guo, M. Cheng, P. Huang, X. Cao, and C. Wang, "Pairwise registration of TLS point clouds using covariance descriptors and a non-cooperative game," *ISPRS J. Photogramm. Remote Sens.*, vol. 134, pp. 15–29, Dec. 2017.

[32] Y. Zang, B. Yang, J. Li, and H. Guan, "An accurate TLS and UAV image point clouds registration method for deformation detection of chaotic hillside areas," *Remote Sens.*, vol. 11, no. 6, p. 647, 2019.

MAOHUA LIU received the B.S. and M.S. degrees in geographic information systems from Liaoning Technical University, in 2003 and 2006, respectively. He is currently pursuing the Ph.D. degree in land resources and information technology with Shenyang Agricultural University, Liaoning, China.

From 2006 to 2016, he hosted and participated in more than ten provincial-level projects and served more than 40 local construction projects. He is currently an Associate Professor with Shenyang Jianzhu University, China. He is an Editor-in-Chief of three teaching materials. He has published more than 20 academic articles in core journals at home and abroad, and applied for three software copyrights.

Mr. Liu received the second prize of the Provincial Natural Science Academic Achievement Award, and the third prize of Shenyang Natural Science Academic Achievement.

XIUBO SUN received the B.S. and M.S. degrees in geographic information systems from Liaoning Technical University, in 2003 and 2006, respectively.

He presided over the science and technology project by the Natural Resources Department of Liaoning Provincial. He published more than ten articles. He received the Liaoning Provincial Science and Technology Progress Award of Surveying and Mapping and the second prize of the Provincial Natural Science Academic Achievement Award.

YAN WANG received the B.S. and M.S. degrees in measurement engineering from Hohai University.

He participated in more than ten vertical projects at the provincial, municipal, and school levels, and presided over or participated in more than forty horizontal projects. He published more than ten academic papers, edited two textbooks, participated in five textbooks, and obtained six software copyrights.

Mr. Wang received the second prize of the Basic Education Contest of Shenyang Construction University, in 2010. In 2014, he received the second prize of the Young Teachers' Teaching Competition of Shenyang Jianzhu University and in 2015, he received the third prize of the Teaching Excellence Award of Shenyang Jianzhu University.

YUE SHAO received the B.S. degree in surveying and mapping engineering from the City Institute Dalian University of Technology, China, in 2017, and the M.S. degree in construction and civil engineering from Shenyang Jianzhu University, China, in 2020. Her research interests are in airborne LiDAR and spectral imaging technology applications.
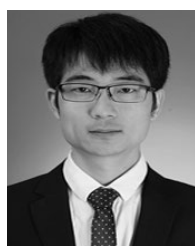
YINGCHUN YOU received the B.S. degree in surveying and mapping engineering and the M.S. degree in road and railway from Shenyang Jianzhu University, in 2007 and 2014, respectively.

He is involved in measuring laboratory instrument management, maintenance, maintenance and laboratory internship guidance. He has undertaken the teaching work of the Engineering Measurement and Real Estate Measurement courses, actively explored teaching methods, and participated in a number of scientific research activities. The work is serious and responsible, and the teaching effect is good.

• • •